

Hydrogen diffusion in C_1' phase clathrate hydrate

Zixuan Song(宋姿璇), Ziyue Zhou(周子岳), Yanwen Lin(林演文), Qiao Shi(石桥), Yongchao Hao(郝勇超), Yuequn Fu(付越群), Zhisen Zhang(张志森), and Jianyang Wu(吴建洋)
Citation: Chin. Phys. B, 2023, 32 (**6**): 066602. DOI: 10.1088/1674-1056/accd4b
Journal homepage: http://cpb.iphy.ac.cn; http://iopscience.iop.org/cpb

What follows is a list of articles you may be interested in

Strain effects on Li^+ diffusion in solid electrolyte interphases: A molecular dynamics study

Xiang Ji(姬祥) and Junqian Zhang(张俊乾)
Chin. Phys. B, 2023, 32 (**6**): 066601. DOI: 10.1088/1674-1056/ac9606

Beryllium carbide as diffusion barrier against Cu: First-principles study

Hua-Liang Cao(曹华亮), Xin-Lu Cheng(程新路), Hong Zhang(张红)
Chin. Phys. B, 2020, 29 (**1**): 016601. DOI: 10.1088/1674-1056/ab593e

A diffusion model for solute atoms diffusing and aggregating in nuclear structural materials

Quan Song(宋泉), Fan-Xin Meng(孟繁新), Bo-Yuan Ning(宁博元), Jun Zhuang(庄军), Xi-Jing Ning(宁西京)
Chin. Phys. B, 2017, 26 (**12**): 126601. DOI: 10.1088/1674-1056/26/12/126601

Crystallization of amorphous silicon beyond the crystallized polycrystalline silicon region induced by metal nickel

Dongli Zhang(张冬利), Mingxiang Wang(王明湘), Man Wong(王文), Hoi-Sing Kwok(郭海成)
Chin. Phys. B, 2017, 26 (**1**): 016601. DOI: 10.1088/1674-1056/26/1/016601

Collective diffusion in carbon nanotubes: Crossover between one dimension and three dimensions

Pei-Rong Chen(陈沛荣), Zhi-Cheng Xu(徐志成), Yu Gu(古宇), Wei-Rong Zhong(钟伟荣)
Chin. Phys. B, 2016, 25 (**8**): 086601. DOI: 10.1088/1674-1056/25/8/086601

SPECIAL TOPIC — Celebrating the 100th Anniversary of Physics Discipline of Xiamen University

Hydrogen diffusion in C_1' phase clathrate hydrate

Zixuan Song(宋姿璇)[1], Ziyue Zhou(周子岳)[1], Yanwen Lin(林演文)[1], Qiao Shi(石桥)[1], Yongchao Hao(郝勇超)[1], Yuequn Fu(付越群)[2], Zhisen Zhang(张志森)[1,†], and Jianyang Wu(吴建洋)[1,3,‡]

[1] *Department of Physics, Research Institute for Biomimetics and Soft Matter, Jiujiang Research Institute and Fujian Provincial Key Laboratory for Soft Functional Materials Research, Xiamen University, Xiamen* 361005, *China*

[2] *PoreLab, the Njord Centre, Department of Physics, University of Oslo, Oslo* 0313, *Norway*

[3] *NTNU Nanomechanical Laboratory, Norwegian University of Science and Technology (NTNU), Trondheim* 7491, *Norway*

(Received 16 February 2023; revised manuscript received 28 March 2023; accepted manuscript online 16 April 2023)

Recently, a new phase C_1' H_2 hydrate was experimentally identified. In this work, the diffusive behaviors of H_2 in C_1' phase clathrate hydrate are explored using classic molecular dynamics (MD) simulations. It reveals that the cage occupancy by H_2 molecule negligibly influences the C_1' phase clathrate structure but greatly dictates the diffusion coefficient of H_2 molecule. Due to the small cage size and small windows connecting the neighboring cages in C_1' phase clathrate, non-occupancy of the neighboring cages is demanded to enable the diffusion of H_2 molecule that is primarily dominated by hopping mechanism. Moreover, the analysis of diffusive free energy landscape reveals lower energy barrier of H_2 molecule in C_1' phase clathrate hydrate than that of other gases in conventional clathrate hydrates, and that H_2 molecule travels through the windows between neighboring cages with preferential molecular orientation. This study provides critical physical insights into the diffusion behaviors of H_2 in the C_1' phase clathrate hydrate, and implies that the C_1' clathrate hydrate is a promising solid structure for the next-generation H_2 storage.

Keywords: clathrate hydrate, hydrogen storage, diffusion, molecular dynamics

PACS: 66.30.Pa, 88.30.R–, 91.50.Hc, 47.11.Mn **DOI:** 10.1088/1674-1056/accd4b

1. Introduction

Hydrogen (H_2) is the most abundant element in the universe and is the basic building block of the universe. It has been attracting a great deal of attention as an essential raw material in innumerable biological and chemical processes.[1,2] It is a remarkable fact that, since the early 1970s when the prices of oil petroleum rose sharply,[3] the possibility of utilization of H_2 as an important alternative fuel has been analyzed rigorously. H_2 is regarded as an ideal energy among new energy resources because of the fact that, when burned, H_2 produces water rather than greenhouse gases such as CO_2. As a result, it is widely accepted that H_2 is one of the most promising fuels for important applications such as vehicles and portable devices within future decades. For practical applications, a mass of materials has been studied for H_2 storage, including metal-organic frameworks, zeolites, carbon-based materials and metal hydrides.[4–16] However, there are a number of challenges in the H_2-use development, such as efficient H_2 production, H_2 storage and transportation.[17–20]

As is known, clathrate hydrates are nonstoichiometric solid compounds made of small molecules and polyhedral cages formed by hydrogen (H)-bonded water molecules under harsh conditions such as low-temperatures and high-pressures.[21–26] From a microscopic perspective, the clathrate water cages entrap the small guest molecules that, however, help to stabilize the cages due to van der Waals (vdW) interactions between the guest and host water molecules.[25,27,28] As a result, clathrate hydrates store small gas molecules at high density.[29] Therefore, clathrate hydrates are being considered as an efficient medium for gas storage and long-distance transportation. In comparison with natural gas hydrates, however, pure H_2 hydrate forms under more stringent conditions such as extreme-low temperatures and high pressures.[28,30,31] For example, Dyadin *et al.*[32,33] reported that a clathrate phase of H_2 hydrate forms in H_2O–H_2 system under conditions of high-pressures of 100 MPa–360 MPa and temperatures of 263 K–283 K. Subsequently, Mao *et al.*[34,35] confirmed that H_2 clathrate hydrate with cubic structure II forms at critical pressure of $\sim$ 220 MPa and critical temperature of $\sim$ 234 K. When the external temperature is reduced to $T = 77$ K, however, such H_2 clathrate hydrate is structurally stable at ambient pressures, while it decomposes with H_2 emission when heated to $\sim$ 140 K.[34] As is indicated, clathrate hydrates can be an important alternative material for H_2 storage and transportation.

Recently, Efimchenko *et al.*[36] synthesized new H_2 hydrate with a trigonal structure, termed as C_0 H_2 hydrate, at pressure of $\sim$ 0.5 GPa and temperature of $\sim$ 253 K. The formation of such new phase C_0 H_2 hydrate at $\sim$ 0.7 GPa and $\sim$ 170 K was further confirmed by Strobel *et al.*[37] More-

†Corresponding author. E-mail: zhangzs@xmu.edu.cn
‡Corresponding author. E-mail: jianyang@xmu.edu.cn

© 2023 Chinese Physical Society and IOP Publishing Ltd

over, clathrate H_2 hydrate that is based on the rhombohedral lattice of proton-ordered ice II formed at $\sim$ 1.2 GPa, named as clathrate 1 (C_1) H_2 hydrate, in which the H_2O molecules are arranged to be a channel-like structure that hosts H_2 molecules.[38–40] With increasing the external pressure, it is able to transform into cubic phase C_2 (the filled ice I_c). Very recently, Wang *et al.*[41] reported a new H_2 clathrate hydrate synthesized at $\sim$ 1.2 GPa and $\sim$ 298 K, termed as C_1' H_2 hydrate. This new clathrate phase is the realization of a disordered ice II, in contrast to all others ordered ice structures. This is remarkable in view of the unknown disordered version of ice II. Those important findings shed new lights on the phase diagram of water and water-based clathrates.

The diffusion properties of H_2 molecules are of crucial fundamental knowledge for H_2 storage and transportation by clathrate hydrates because they affects the decay, formation and dissociation kinetics.[42] To date, the diffusion properties of H_2 molecules in hexagonal ice structure and conventional clathrate hydrates were well-investigated both experimentally and theoretically. Experimentally, it was showed via neutron inelastic scattering experiments that the diffusion coefficient of H_2 molecules in deuterated ice at 25 K is measured to be $\sim 1.3 \times 10^{-5}$ cm^2/s that is one order-of-magnitude lower than that of H_2 in liquid H_2 phase ($\sim 1.4 \times 10^{-4}$ cm^2/s).[43] Using pulsed field gradient nuclear magnetic resonance (NMR) technique, Okuchi *et al.*[44] measured directly the diffusion of H_2 in solid hydrate medium, and revealed that the entrapped H_2 molecules are moveable at temperature of 250 K. Moreover, through NMR technique, the collision and diffusion dynamics of dense H_2 in filled-ice I_c hydrogen's hydrate at pressures to 4.6 GPa were investigated, and it was showed that active translational diffusion of H_2 molecules through the leaky H_2O framework of the clathrate hydrate takes place.[45] Theoretically, using molecular dynamics (MD) simulations, Iwai and Hirata[46] investigated the diffusion coefficients of H_2 in binary H_2-THF hydrate formed under various contents of H_2 and THF at temperatures of 300 K and 310 K and pressure of 10.1 MPa, and revealed that H_2 molecules are able to diffuse from cage-to-cage and the diffusion coefficients of H_2 molecules are qualitatively in agreement with previous experimental data. A hydrogen delocalization model and a proposed hydrogen hydrate phase diffusion (HHPD) model were used to analyze the formation mechanisms.[47] Harada *et al.*[48] reported via MD simulations that H_2 molecules diffuse rapidly in C_1 H_2 hydrate.

Those pioneering works indicate the important implications of efficient H_2-storage by H_2O-based crystals, however, the fundamental knowledge such as detailed diffusion mechanism in dense H_2O-based crystals has not been well-understood. In this work, the diffusion behaviors of H_2 molecule in recently experimentally-synthesized C_1' clathrate hydrate[41] are explored using classic MD simulations,[49–58] focusing on the effects of cage occupancy,[59–62] as well as the free-energy landscapes. The outcomes of this study provide important insights into the diffusion of H_2 in C_1' phase clathrate hydrate, which is of help for H_2 gas purification, storage and transport by water-based clathrate structures.

2. Model and methodology

In this study, very recently experimentally-identified C_1' H_2 hydrate[41] is taken into investigation. The top-view of unit-cell of C_1' H_2 hydrate is shown in Fig. 1(a). As shown in Fig. 1(a), C_1' H_2 hydrate is a rhombohedral crystal with space group $R\bar{3}c$. Its unit-cell has lattice constants of $a = b =$ 12.984 Å, $c = 6.243$ Å, and consists of 36 H_2O molecules. Figure 1(b) shows one side-view of unit-cell of C_1' H_2 hydrate, in which two hexagonal channels formed by columns of alternating puckered and flat rings are highlighted to entrap H_2 guest molecules. The hexagonal channel with unit-cell length consists of 2 H-bonded hexamers including one chair-form and one almost flat, as shown in Fig. 1(c).

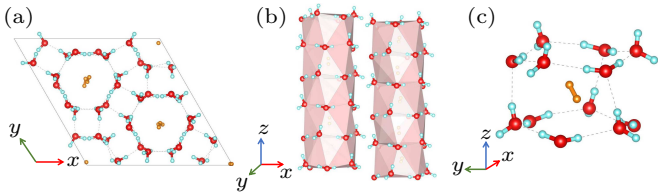


Fig. 1. Molecular model of C_1' H_2 hydrate. (a) Top-view of configuration of primitive cell of C_1' H_2 hydrate. (b) One side-view of configuration of C_1' H_2 hydrate, in which two hexagonal channels formed by clathrate cages in primitive cell of C_1' H_2 hydrate are highlighted. The length vector of hexagonal channels is along z-axis. (c) Structural motif of a clathrate cage formed by hydrogen-bonded water molecules for C_1' H_2 hydrate, in which a H_2 guest molecule is entrapped in the clathrate cages. Orange, red and bluish spheres indicate the hydrogen, oxygen and hydrogen from H_2 guest and water molecules, respectively, while the gray dash lines indicate the hydrogen bonds formed by water molecules.

Here, a supercell of $3 \times 4 \times 5$ unit-cells is generated for examining the diffusion properties of H_2 in the C_1' H_2 hydrate. The as-generated C_1' H_2 hydrate contains 720 H_2O molecules and 120 H_2 molecules in the simulation box. For the initial configuration of as-generated C_1' H_2 hydrate, H_2O molecules are arranged to follow the Bernal–Fowler rule.[63] To reveal the effect of cage occupancy on the guest diffusion behaviors, C_1' H_2 hydrates with vacancy of guest H_2 molecule varying from 0%–100% are constructed. Moreover, five samples of C_1' H_2 hydrates with one given occupancy rate of cages are generated by randomly removing H_2 guest molecules with different random seeds for capturing the diffusion properties of H_2 guest molecule.

The TIP4P/Ice forcefield[6] is used to describe the host H_2O molecules of C_1' H_2 hydrates, in which the O–H bonds in the water model are fixed using the linear constraint solver (LINCS) algorithm.[64] For guest H_2 molecules, all-atom

model is also considered, in which the bond stretch in H_2 molecule is described by a harmonic potential.[65] Those potentials are previously adopted to mimic H_2 hydrates.[66,67] The atomic interaction of inter-molecules in C_1' H_2 hydrates is described by combining a Lennard–Jones potential with a Coulomb term to account for the vdW and electrostatic interactions.

Prior to MD simulations, all the configurations of as-constructed C_1' H_2 hydrate are firstly energy-minimized. Then, MD relaxations of energy-minimized samples are carried out for 0.5 ns at temperature of 298 K and confining pressure of 1.2 GPa under NPT ensemble, corresponding to the thermodynamic conditions of Raman spectroscopy and theoretical calculations where the H-disordered nature of C_1' H_2 hydrate is found.[41] Finally, MD simulations are performed at 298 K for 50 ns for production, in which the configurations and trajectory during the MD simulations are collected for analysis. During the MD simulations, the atomic motions in the C_1' H_2 hydrate systems follow the classic Newton's motion equation that is solved by the velocity-Verlet algorithm with timestep of 1.0 fs. All the MD calculations are implemented using the GROMACS 4.6.7 package.[68]

Moreover, to further uncover the diffusion mechanisms of H_2 molecule in the C_1' H_2 hydrate, the diffusion energy barrier is calculated. Here, two-dimensional (2D) free-energy landscapes of guest H_2 molecules in the C_1' H_2 hydrate are computed using the meta-dynamics method[69,70] that is implemented in GROMACS 4.6.7 with PLUMED 2.2.3.[68] In the calculations, walls are imposed to enhance the sampling, in which the force constant of the walls is set to 100 kJ·mol^{-1}·nm^{-2}. In the meta-dynamic simulations, the width and the height of the Gaussian hills are assigned to be 0.06 and 0.1 kJ·mol^{-1}, respectively. The output frequency of the hill addition is set to be 500 timesteps.

3. Results and discussion

3.1. Radial distribution functions

The radial distribution functions (RDFs)/$g(r)$ are an important metric to characterize the structural order of materials, as well as to describe how the density of surrounding particle varies as a function of distance from a tagged particle. Here, to evaluate the molecular structure of C_1' H_2 hydrate, the RDFs profiles of as-relaxed structures of C_1' H_2 hydrate are computed. Figure 2(a) shows the RDF profiles of oxygen atoms of water molecules (O_W–O_W) in C_1' H_2 hydrate with cage occupancy varying from 10%–100%. At short distances ($r < 2.3$ Å), $g(r)$ is zero, stemming from the presence of very strong repulsive forces between inter-molecules of water at short distances. It is observed that the first peak of $g(r)$ profile occurs at $\sim$ 2.78 Å, similar to other hydrate crystals.[71] Such peak indicates that a large number of the neighboring oxygen atoms in host water molecules show atomic distance of $\sim$ 2.78 Å. The second peak situates at $r \simeq 3.5$ Å. Such two significant peaks indicate the tetrahedral hydrogen bond network of water molecules in C_1' H_2 hydrate. The following weak peak is due to the presence of six-member water rings in C_1' H_2 hydrate. By comparison, as the cage occupancy varies from 10%–100%, the RDF profiles of C_1' H_2 hydrate are almost overlapping, suggesting that the absence of guest H_2 molecule plays negligible role in the changing of cage structures.

Figure 2(b) shows the computed RDF profiles of oxygen and hydrogen atoms of water molecules (O_W–H_W) of C_1' H_2 hydrate. Within the distance range of 0 Å–4.0 Å, three main peaks are observed in the RDF profiles. The first peak locates at $r \simeq 1.0$ Å, which corresponds to the bond distance of O–H in water molecules. The second peak situates at $r \simeq 1.7$ Å, indicating the average length of H-bonds formed in C_1' H_2 hydrate. The third peak positioning at $r \simeq 3.1$ Å suggests the distance between hydrogen and oxygen atoms that is separated by a water molecule for the four- and six-member rings in C_1' H_2 hydrate. Figure 2(c) shows the RDF profile of water oxygens atoms — guest hydrogen atoms (O_w–H_H). The first peak locates at $r \simeq 3.1$ Å, corresponding to the mean nearest distance between host water oxygen atoms and guest hydrogen molecules. The second and third peaks locate at $r \simeq 5.9$ Å and 8.3 Å, respectively, which can be attributed to the distance between oxygen atoms in neighboring host water cage and guest hydrogen molecules.

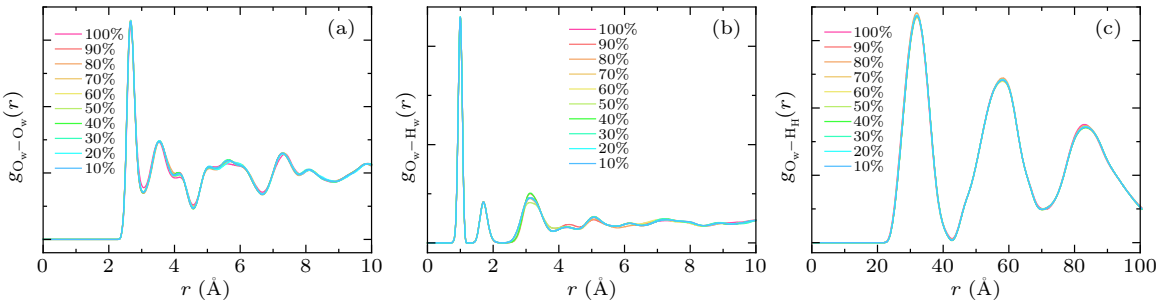


Fig. 2. Radial distribution functions (RDFs) profiles in relaxed C_1' H_2 hydrate with vacancy of guest H_2 molecule varying from 10%–100%. (a) RDF profiles of oxygens of water host molecules (O_w–O_w). (b) RDF profiles of oxygen–hydrogen of water host molecules (O_w–H_w). (c) RDF profiles of oxygen–hydrogen (O_W–H_H), where the oxygen and hydrogen are from host water and guest H_2 molecules, respectively.

3.2. Orientation of H_2 molecule

As is known, translational and rotational mobility of guest molecules in clathrate hydrates is strongly limited due to the fact that guest molecules are confined into clathrate cages formed by host water molecules. Here, the orientation distribution of H_2 guest molecule in the cages of C_1' H_2 hydrate is examined. As illustrated in the inset of Fig. 3, the orientational angle (ϕ) of guest H_2 molecule is defined by the angle between the orientational vector of H_2 guest molecules and the length vector (the vector in the z-axis) of the hexagonal channels formed by H_2O water molecules (Fig. 1(b)). Figure 3 displays the distribution probability of the orientational angle (ϕ) of H_2 guest molecule ($P(\phi)$) for relaxed C_1' H_2 hydrate in which all clathrate cages are fully occupied by H_2 guest molecule. Apparently, it is observed that non-uniformed $P(\phi)$ of H_2 guest molecule confined in the clathrate cages of C_1' H_2 hydrate. Such non-uniformed $P(\phi)$ of H_2 guest molecule indicates that there exists preferential orientation of H_2 guest molecule due to the unique geometrical clathrate cage. Remarkably, maximum $P(\phi)$ of orientational configuration of H_2 guest molecule occurs at $\phi \simeq 80^\circ$ in the clathrate cage. This suggests that H_2 guest molecule almost tends to orient to length direction of the clathrate cages-formed hexagonal channels, yet with small angle of deviation to the length direction.

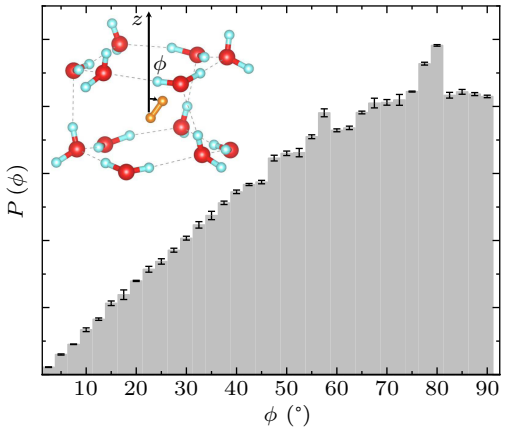


Fig. 3. Orientational probability of guest H_2 molecule of clathrate cages in C_1' H_2 hydrate in which the clathrate cages are fully occupied by guest H_2 molecules. The insert illustration indicates the definition of orientational angle (ϕ) of guest H_2 molecules confined in the clathrate cages.

3.3. Diffusion of H_2 molecule

As is known, mean square displacement (MSD) of atoms/molecules describes the average distance travelled by the atoms/molecules from a reference position within a certain time,[72] and it therefore quantitatively measures the deviation of the position of atoms/molecules with respect to one reference position over time. To examine the diffusion properties, the MSD of guest H_2 molecules in C_1' H_2 hydrate with cage occupancy of 10% is computed. Figure 4 presents the simulated MSD of guest H_2 molecules in C_1' H_2 hydrate as a function of time. The MSDs along x-, y-, and z-axes are denoted as $|\Delta \boldsymbol{r}(t)_x|^2$, $|\Delta \boldsymbol{r}(t)_y|^2$, and $|\Delta \boldsymbol{r}(t)_z|^2$, respectively, while the total MSD (namely the 3-dimentional MSD, $|\Delta \boldsymbol{r}(t)|$) is calculated as follows:

$$|\Delta \boldsymbol{r}(t)|^2 = |\Delta \boldsymbol{r}(t)_x|^2 + |\Delta \boldsymbol{r}(t)_y|^2 + |\Delta \boldsymbol{r}(t)_z|^2. \quad (1)$$

As is seen in Fig. 4, the MSD–t profiles show linear functions, suggesting pure free diffusion yet no confined diffusion or flow plus diffusion. However, the values of MSD are strongly direction-dependent, indicating highly anisotropic diffusion of guest H_2 molecules within the C_1' H_2 hydrate. Guest H_2 molecule shows similar MSD values along x- and y-axes, while the MSD value along z-axis is around two order-of-magnitudes of those along x- and y-axes. This indicates that the travelling of guest H_2 molecules primarily occurs along the hexagonal channels, which could be regarded as one-dimensional (1D) diffusion.

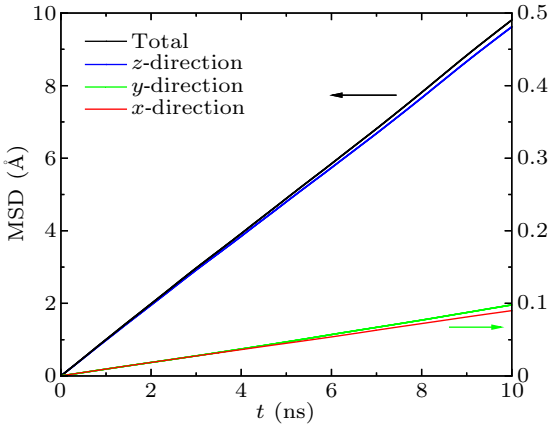


Fig. 4. Mean square displacement (MSD) of guest H_2 molecule in C_1' H_2 hydrate with cage occupancy of 10%, in which the red, green and blue curves represent MSD of the tagged H_2 molecule in the x, y, and z-axes, while the total MSD is described by the black curve.

The effects of cage occupancy on the diffusion properties of guest H_2 molecule in C_1' hydrate are also investigated. Figure 5(a) shows that variations in the values of MSD of guest H_2 molecules with simulation time for C_1' H_2 hydrate with cage occupancy varying from 10%–100%. It is observed that C_1' H_2 hydrate with cage occupancy of 10%–100% shows linear curves of MSD–t. However, the MSD values of guest H_2 molecules are different from each other. C_1' H_2 hydrate with high cage occupancy shows small MSD values, indicating weak diffusion ability of guest H_2 molecules.

As is known, for the simplest diffusion case system, the probability density of the particle displacement $|\Delta \boldsymbol{r}(t)|$ can be described by the Gaussian distribution. When fluid particles are confined in 1D channels with small enough diameter, however, the movement of the fluid particles is constrained to one direction and the particles are not able to pass their neighbors. As a result, the 1D random walk of the fluid particles gives rise

to a relationship of $|\Delta \boldsymbol{r}(t)|^2 \propto t^{1/2}$. Once this relationship is violated, the diffusion in such case becomes anomalous.[73,74] Thus, the relationship of MSD–t follows the nonlinear function as

$$|\Delta \boldsymbol{r}(t)|^2 = K(\boldsymbol{r})t^{\alpha}, \tag{2}$$

where $K(\boldsymbol{r})$ is generalized diffusion coefficient. When $0 < \alpha < 1$, a sub-diffusion behavior is indicated in the case, while a super-diffusion behavior arises as $\alpha > 1$. In this study, as is shown in Fig. 5(a), the values of MSD of guest H_2 molecules in C_1' H_2 hydrate increase linearly with simulation time, although guest H_2 molecules are confined in hexagonal water-based channels of C_1' H_2 hydrate, indicating normal diffusion behavior, yet non-sub-diffusion or non-super-diffusion. The diffusion of guest H_2 molecules in C_1' H_2 hydrate can be characterized as being Fickian.[75] Observing the curve in the image, it can be seen that with the increase of vacancy number and the decrease of cage occupancy, the slope of MSD decreases successively.

To quantitatively evaluate the diffusion properties, the diffusion coefficient (D) of guest H_2 molecules in C_1' hydrate can be determined by Einstein equation[76] as follows:

$$\lim_{t\to\infty}\langle \|\boldsymbol{r}_i(t) - \boldsymbol{r}_i(0)\|^2\rangle_{i\varepsilon A} = 2nDt, \tag{3}$$

where $\boldsymbol{r}_i(0)$ and $\boldsymbol{r}_i(t)$ are the positional vectors of the particle i at $t = 0$ and a given time t. Here, $n = 1$ due to one dimensional diffusion of H_2 in the C_1' hydrate. Figure 5(b) shows the variation in the D with t for guest H_2 molecules in C_1' H_2 hydrate with cage occupancy from 0%–100%. When cage occupancy is 100%, D of guest H_2 molecules is extremely small because all the guest H_2 molecules are not able to diffuse to neighboring clathrate cages and thermally-vibrate only within confined clathrate cages. When cage occupancy of C_1' H_2 hydrate varies from 10%–90%, D of guest H_2 molecules monotonically increases with decreasing the cage occupancy. Note that the hydrate systems with cage occupancy of 10% and 20% show large errors in the D due to limit number of guest H_2 molecules that travel in the hexagonal channels.

Table 1 lists the D of H_2 molecules in different systems. It is found that the D of H_2 molecule in the C_1' hydrate is predicted to be $\sim 8.0\times10^{-8}$–19.0×10^{-8} $cm^2{\cdot}s^{-1}$, depending on the cage occupancy. At high cage occupancy, the predicted D of H_2 molecule in C_1' hydrate is similar to that in sII tetrahydrofuran (THF) and C_1 clathrate hydrates calculated/measured from previous studies[44,47,48,77] using MD/NMR techniques. However, the D of H_2 molecule in C_1' hydrate is predicted to be two and three orders-of-magnitude lower than that in hexagonal D_2O ice (I_h) and liquid hydrogen using quasi-elastic neutron scattering (QENS),[78,79] respectively.

Table 1. Diffusion coefficients (D) of H_2 molecule in different systems obtained by MD, NMR, and QENS techniques.

System	Temperature (K)	D (cm^2/s)	Technique	Refs.
C_1' hydrate	298	8.0×10^{-8}–19.0×10^{-8}	MD	this work
Hexagonal D_2O ice	25	1.3×10^{-5}	QENS	[78]
	43	7.5×10^{-5}		
	60	9.5×10^{-5}		
Liquid hydrogen	20.75	1.075×10^{-4}	QENS	[79]
sII THF hydrate	265	1.6×10^{-8}	NMR	[44]
sII THF hydrate	300	9.8×10^{-8}	MD	[47]
C_1 hydrate	291	1.2×10^{-8}	NMR	[77]
C_1 hydrate	291	8.6×10^{-8}	MD	[48]

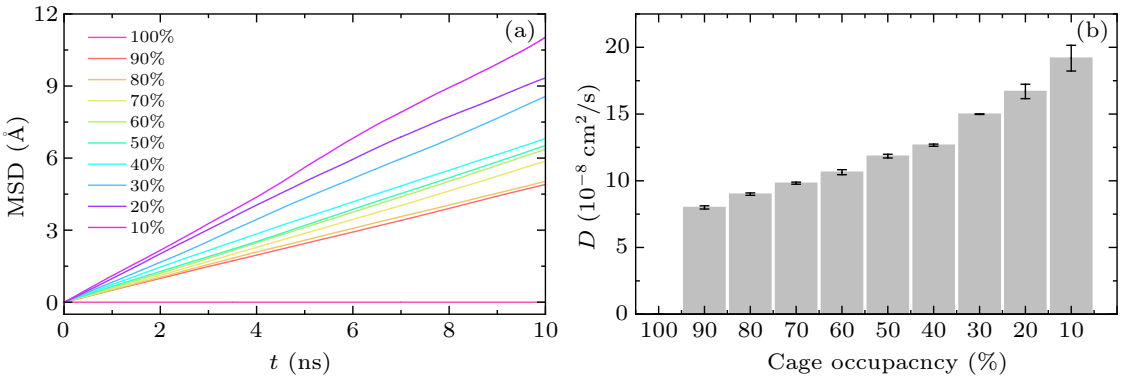


Fig. 5. Diffusion properties of guest H_2 molecules in C_1' H_2 hydrate. (a) Mean square displacement (MSD) of guest H_2 molecules in C_1' H_2 hydrate with cage occupancy varying from 10%–100% as function of simulation time. (b) Variation in the diffusion coefficient (D) of guest H_2 molecules in C_1' H_2 hydrate with cage occupancy.

3.4. Hoping diffusion mechanism of H_2 molecule

To further uncover the diffusion behaviors of guest H_2 molecules in C_1' H_2 hydrate, the snapshots of the molecular configurations of C_1' H_2 hydrate are captured during the MD simulations. Figure 6 presents the variation in the z-positions of guest H_2 molecules in a hexagonal channel of C_1' H_2 hydrate with cage occupancy of 90% with simulation time, as well as molecular motif of water based-hexagonal channel composed of 10 cages at simulation time of 0 ns, in which 9 cages are occupied by H_2 molecules. As is seen from the position curves of H_2 molecules in Fig. 6, the z-position of bottom H_2 molecule that is neighbored by one H_2 molecule-occupied cage and one guest-free cage firstly changes suddenly from $z \simeq 0.466$ nm to 0.152 nm at $t \simeq 0.14$ ns. Such sudden change of z-position clearly illustrates that the H_2 molecule diffuses in the hexagonal channel via hopping mechanism. Note that before the hopping time, other H_2 molecules that are neighbored by H_2 molecules-occupied cages remain their initial z-positions. This infers that the guest-free neighboring cages are the requirement for the diffusion of a H_2 molecule in the hexagonal channel of C_1' H_2 hydrate, and two or more H_2 molecules cannot occupy the single cage simultaneously. At $t \simeq 1.93$ ns, however, the z-position of the H_2 molecule changes back to $z \simeq 0.444$ nm, but then diffuses downward to guest-free cage. Very soon, due to that the cage is free of occupancy by H_2 molecule, the second bottom H_2 molecule starts to diffuse downward to the guest-free cage. Subsequently, other H_2 molecules diffuse downward step-by-step, achieving the global 1D diffusion of guest H_2 molecules in the hexagonal channel of C_1' H_2 hydrate. Guest H_2 molecules cannot diffuse past their neighboring ones. The step-by-step diffusion mechanism of guest H_2 molecules explains the cage occupancy dependent D. Moreover, during the 1D diffusion process, guest H_2 molecules show several repeats of hopping forward-and-backward within several picoseconds to hundred picoseconds. This indicates that the entrapped time of H_2 molecules within a cage varies from several picoseconds to hundred picoseconds if its neighboring cage is guest-free.

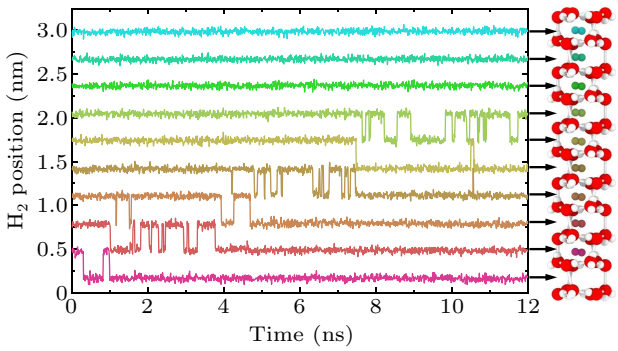


Fig. 6. The z-positions of guest H_2 molecules in a hexagonal channel of C_1' H_2 hydrate as a function of simulation time. The inset is the molecular configuration of a hexagonal channel composed of 10 cages, in which 9 cages are occupied by guest H_2 molecules. For clarification, there is one-to-one correspondence in the painting colors between the solid lines and the guest H_2 molecules.

3.5. Energy barrier of H_2 diffusion

Potential of mean force (PMF) calculations is performed to characterize the change in the free-energy as guest H_2 molecules diffuse through the hexgaonal channel of C_1' H_2 hydrate. For transition of state from 0 to 1 in a system, the gap in the free energy between the two states can be determined using the density probability distribution of the system in the two states as follows:[80]

$$\Delta G = G_1 - G_0 = -k_B T \ln \frac{\rho_1}{\rho_0}, \tag{4}$$

where G, k_B, and T are the Gibbs free energy, Boltzmann constant and temperature, respectively. ρ_0 and ρ_1 are the density probability at states 0 and 1, respectively. In this study, the PMF profiles of C_1' H_2 hydrate with different cage occupancies are calculated. It is found that, excluding C_1' H_2 hydrate with cage occupancy of 100%, the PMF profiles of C_1' H_2 hydrate with cage occupancy varying from 10%–90% are pretty similar. This indcates that when C_1' H_2 hydrate has cage occupancy of 10%–90%, the cage occupancy shows negligible effect on the free energy of H_2 molecules diffusing in the hexgonal channels of C_1' H_2 hydrate.

Figure 7(a) shows the density probability distribution of guest H_2 molecules in C_1' H_2 hydrate, as well as the PMF (1D free energy landscape) as a function of z-position for guest H_2 molecules diffusing in the hexgonal channels of C_1' H_2 hydrate that is determined by the density probability distribution using Eq. (4). The maxima and minima of 1D free energy landscape locate at the cage junction and the cage cavity, respectively. Based on the PMF profiles, the ΔG for cage-to-cage diffusion of guest H_2 molecule is detemined to be $\sim 4.32 \pm 0.047$ kJ/mol. However, the method for calculating PMF profiles using the data of the density probability distributions is usually not robust because of inadequate sampling at specific distances, thereby resulting in quasi-nonergodicity. Moreover, the PMF profile strongly depends upon the bin size chosen to construct the density probability distribution. As a result, there can be a relatively large error to determine the PMF profile using the data of density probability distribution.

Therefore, to accurately characterize the ΔG of guest H_2 molecules diffusion through the hexagonal channels, 2D free-energy landscape of guest H_2 molecules is further calculated. Figure 7(b) shows the free-energy landscape as a function of z-position and molecular orientation of guest H_2 molecule confined in the hexagonal channel of C_1' H_2 hydrate with cage occupancy of 10%. As is indicated in Fig. 7(a), the 2D free-energy landscape of molecular orientation of H_2 molecules exhibits a periodic structure along the z-axis, with the maximum and minimum values situated at the junction of two cages and inside of the cage cavity. The gap between the maximum and minimum values is determined to be $\sim 6.36 \pm 0.16$ kJ/mol.

The 2D free energy minima locates at $\phi \simeq 80^\circ$ in this system, which is consistent with the result of $P(\phi)$ in Fig. 3. Apparently, this 2D ΔG of H_2 molecules diffusion in C_1' H_2 is higher than 1D ΔG predicted by the density probability distribution. Table 2 lists the ΔG of various gases travelling through ice-based systems. It is found that the ΔG of gases in clathrate systems varies with the clathrate structure, meaured method and external conditions. By comparison, it is identified that there is lower ΔG of H_2 molecule diffusing in C_1' hydrate than that of CH_4, CO_2 and air in sI and sII clathrate hydrates.[81–84] For the case of H_2 molecule, however, the ΔG of H_2 molecule diffusing in C_1' hydrate falls in the wide range of that in sII hydrate. Moreover, the ΔG of H_2 molecule diffusing in C_1' hydrate is predicted to be lower than that in sI hysdrate.

Table 2. Energy barrier (ΔG) of gases diffusing in ice-based systems.

System	Gases	ΔG (kJ/mol)	Technique	Refs.
C_1' hydrate	H_2	6.36 ± 0.16	MD	this work
sII hydrate	H_2	3 ± 1	NMR	[44]
		23–28	electronic-structure calculations	[85]
		32 ± 12	MD	[86]
sII hydrate	CH_4	52.1	neutron diffraction measurements	[81]
sII hydrate	CO_2	54.6	neutron diffraction measurements	[82]
sII hydrate	air	50	raman spectra measurements	[83]
sI hydrate	H_2	18.0	CCSD(T)/aug-cc-pVTZ	[84]
	CH_4	82.4		
	CO_2	27.8		

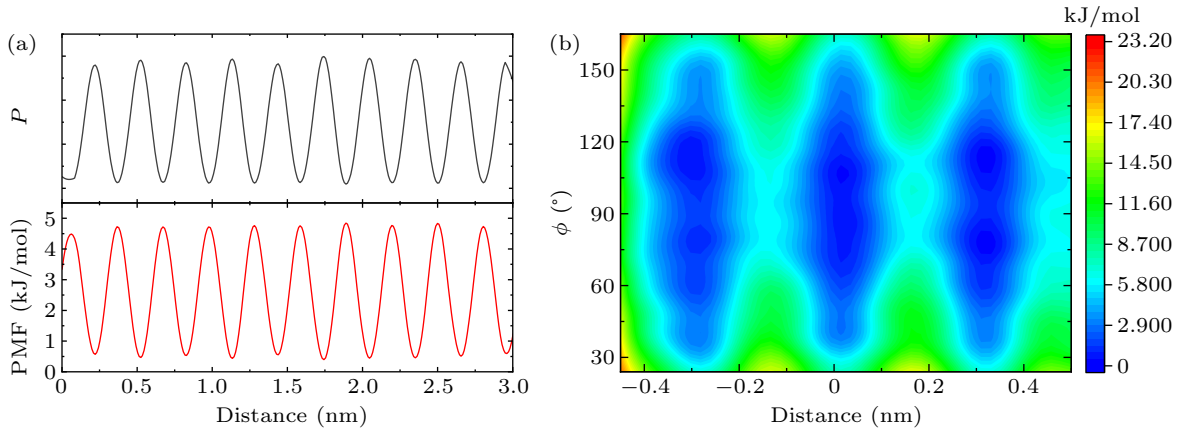


Fig. 7. Free-energy barrier (ΔG) of H_2 molecule in C_1' H_2 hydrate with 10% cage occupancy. (a) Density probability of guest H_2 molecule in the C_1' H_2 hydrate, and potential of mean force (PMF) of guest H_2 molecule in C_1' H_2 hydrate as a function of z-position of H_2 molecule. (b) 2D ΔG of guest H_2 molecule in C_1' H_2 hydrate as a function of z-position and molecular orientation of H_2 molecule.

4. Conclusion

Extensive classic MD simulations are performed to examine the diffusion behaviors of H_2 molecule in recently-identified novel C_1' phase clathrate hydrate. The structural properties of C_1' H_2 hydrate are analysized by the RDF profiles and $P(\phi)$ of H_2 molecule. It is found that there is negligible effect of cage occupancy by H_2 molecule on the clatrhate structure, and H_2 molecule shows perferential molecular orientaion with $\phi \simeq 80^\circ$. As a result of the presence of unique channel structures in C_1' hydrate, there is strongly anisotropic diffusion of H_2, with perferential diffusion along the channels, and the diffusion can be characterized as being Fickian, with hopping diffusion mechanism. The D of H_2 in C_1' hydrate varies from 8.0×10^{-8}–19.0×10^{-8} cm^2/s, and is monotonically increased with decreasing the cage occupancy, which is beneficial for the formation of C_1' H_2 hydrate in terms of the formation kinetics. The non-occupancy of the neighboring cage is the critical requirement to enable the H_2 diffusion. Moreover, the calculation of 2D free-energy landscapes as a function of molecular orientation and the position of z-axis uncovers that H_2 in C_1' phase hydrate possesses comparable ΔG in sII hydrate, but lower diffusion ΔG than other gases such as CH_4, CO_2 and air in sI and sII clathrate hydrates. By comparing with that of sI and sII clathrate hydrates, C_1' phase hydrate is a good media for long-distance H_2-storage and transportation. Moreover, there is critcal molecular orientaion of H_2 when diffusing through the windows connecting the neighboring cages.

Acknowledgments

Project supported by the National Natural Science Foundation of China (Grant Nos. 12172314, 11772278, and 11904300), the Jiangxi Provincial Outstanding Young Talents Program (Grant No. 20192BCBL23029), the Fundamen-

tal Research Funds for the Central Universities (Xiamen University: Grant Nos. 20720210025 and 20720220023), the Research Council of Norway (Grant No. 262644), and the 111 project (Grant No. B16029). Shaorong Fang and Tianfu Wu from Information and Network Center of Xiamen University are acknowledged for the help with the high-performance computer.

References

[1] Florusse L J, Peters C J, Schoonman J, Hester K C, Koh C A, Dec S F, Marsh K N and Sloan E D 2004 *Science* **306** 469
[2] Veluswamy H P, Kumar R and Linga P 2014 *Appl. Energy* **122** 112
[3] von Helmolt R and Eberle U 2007 *J. Power Sources* **165** 833
[4] Schlapbach L and Zuttel A 2001 *Nature* **414** 353
[5] Zuttel A 2004 *Naturwissenschaften* **91** 157
[6] Abascal J L, Sanz E, Garcia F R and Vega C 2005 *J. Chem. Phys.* **122** 234511
[7] Nijkamp M G, Raaymakers J E M J, van Dillen A J and de Jong K P 2001 *Appl. Phys. A* **72** 619
[8] Darkrim L F, Malbrunot P and Tartaglia G P 2002 *Int. J. Hydrog. Energy* **27** 193
[9] Seayad A M and Antonelli D M 2004 *Adv. Mater.* **16** 765
[10] Snurr R Q, Hupp J T and Nguyen S T 2004 *AIChE J.* **50** 1090
[11] Rowsell J L and Yaghi O M 2005 *Angew. Chem. Int. Ed.* **44** 4670
[12] Dinca M, Dailly A, Liu Y, Brown C M, Neumann D A and Long J R 2006 *J. Am. Chem. Soc.* **128** 16876
[13] Ströbel R, Garche J, Moseley P T, Jörissen L and Wolf G 2006 *J. Power Sources* **159** 781
[14] Collins D J and Zhou H C 2007 *J. Mater. Chem.* **17** 3154
[15] Pan H Z, Wang Y L, He K H, Wei M Z, Ouyang Y and Chen L 2013 *Chin. Phys. B* **22** 067101
[16] Bhihia M, Lakhala M, Labrimb H, Benyoussefa A, Kenza A E, Mounkachic O and Hlile E K 2012 *Chin. Phys. B* **21** 097501
[17] Wang L F and Yang R T 2008 *Energy Environ. Sci.* **1** 268
[18] Thomas K M 2009 *Dalton Trans.* **9** 1487
[19] Züttel A 2003 *Mater. Today* **6** 24
[20] Jinzhe L, Lider A M and Kudiiarov V N 2019 *Chin. Phys. B* **28** 98801
[21] Koh C A, Sloan E D, Sum A K and Wu D T 2011 *Annu. Rev. Chem. Biomol. Eng.* **2** 237
[22] Ning F L, Yu Y B, Kjelstrup S, Vlugt T J H and Glavatskiy K 2012 *Energy Environ. Sci.* **5** 6779
[23] Hassanpouryouzband A, Joonaki E, Vasheghani F M, Takeya S, Ruppel C, Yang J, English N J, Schicks J M, Edlmann K, Mehrabian H, Aman Z M and Tohidi B 2020 *Chem. Soc. Rev.* **49** 5225
[24] Hammerschmidt E G 2002 *Ind. Eng. Chem.* **26** 851
[25] Uchida T, Ohmura R and Hori A 2008 *J. Phys. Chem. C* **112** 4719
[26] Liu Z B, Dong S L and Lin W 2008 *Chin. Phys. Lett.* **25** 2680
[27] Torres T A, Kroon M C, Peters C J, Moudrakovski I L, Ratcliffe C I, Alavi S and Ripmeester J A 2014 *J. Chem. Phys.* **140** 214703
[28] Xu K, Lin Y W, Li T, Fu Y Q, Zhang Z S and Wua J Y 2022 *J. Mol. Liq.* **347** 118391
[29] Lenz A and Ojamae L 2011 *J. Phys. Chem. A* **115** 6169
[30] Shi Q, Cao P Q, Han Z D, Ning F L, Gong H, Xin Y, Zhang Z S and Wu J Y 2018 *Cryst. Growth Des.* **18** 6729
[31] Guo P, Qiu Y L, Li L L, Luo Q, Zhao J F and Pan Y K 2018 *Chin. Phys. B* **27** 43103
[32] Dyadin Y A, Larionov E G, Manakov A Y, Zhurko F V, Aladko E Y, Mikina T V and Komarov V Y 1999 *Mendeleev Commun.* **9** 209
[33] Dyadin Y A, Aladko E Y, Manakov A Y, Zhurko F V, Mikina T V, Komarov V Y and Grachev E V 1999 *J. Struct. Chem.* **40** 790
[34] Mao W L, Mao H K, Goncharov A F, Struzhkin V V, Guo Q, Hu J, Shu J, Hemley R J, Somayazulu M and Zhao Y 2002 *Science* **297** 2247
[35] Mao W L and Mao H K 2004 *Proc. Natl. Acad. Sci. USA* **101** 708
[36] Efimchenko V S, Kuzovnikov M A, Fedotov V K, Sakharov M K, Simonov S V and Tkacz M 2011 *J. Alloys Compd.* **509** S860
[37] Strobel T A, Ganesh P, Somayazulu M, Kent P R and Hemley R J 2011 *Phys. Rev. Lett.* **107** 255503
[38] Kamb B 1964 *Acta Crystallogr.* **17** 1437
[39] Machida S, Hirai H, Kawamura T, Yamamoto Y and Yagi T 2010 *J. Phys. Chem. Solids* **71** 1324
[40] Fortes A D, Wood I G, Alfredsson M, Vocadlo L and Knight K S 2005 *J. Appl. Crystallogr.* **38** 612
[41] Wang Y, Glazyrin K, Roizen V, Oganov A R, Chernyshov I, Zhang X, Greenberg E, Prakapenka V B, Yang X, Jiang S Q and Goncharov A F 2020 *Phys. Rev. Lett.* **125** 255702
[42] Faizullin M Z, Vinogradov A V and Koverda V P 2014 *High Temp.* **52** 830
[43] Strauss H L, Chen Z and Loong C K 1994 *J. Chem. Phys.* **101** 7177
[44] Okuchi T, Moudrakovski I L and Ripmeester J A 2007 *Appl. Phys. Lett.* **91** 171903
[45] Okuchi T 2012 *J. Phys. Chem. C* **116** 2179
[46] Iwai Y and Hirata M 2012 *Mol. Simul.* **38** 333
[47] Nagai Y, Yoshioka H, Ota M, Sato Y, Inomata H and Smith R L 2008 *AIChE J.* **54** 3007
[48] Harada A, Arman Y and Miura S 2019 *J. Mol. Liq.* **292** 111316
[49] Zhang Y, Zhang R, Lai J Q and Li H 2019 *Acta Phys. Sin.* **68** 224702 (in Chinese)
[50] Shao Y F, Meng F S, Li J H and Zhao X 2019 *Acta Phys. Sin.* **68** 216201 (in Chinese)
[51] Wang Y T, Zeng X G and Yang X 2019 *Acta Phys. Sin.* **68** 246102 (in Chinese)
[52] Zhang C B and Zhou X 2020 *Chin. Phys. B* **29** 108706
[53] Jiang W R, Wang R, Ren X G, Zhang Z Y, Li D H and Wang Z G 2020 *Chin. Phys. B* **29** 103101
[54] Tang Y M, Yao Y F and Wei G H 2020 *Chin. Phys. B* **29** 108710
[55] Zhang Z X, Zhao X Y, Li Y, Cui H, Luo Z C, Xu W C and Luo A P 2020 *Chin. Phys. B* **29** 104208
[56] Wang L Y, Xu X P, Li Z G and Qian T Z 2020 *Chin. Phys. B* **29** 090501
[57] Li T, Li J W, Pang C L, An H L, Geng Y Z and Wang J Q 2020 *Chin. Phys. B* **29** 098701
[58] Wang J L, Dang W Q, Liu D P and Guo Z C 2020 *Chin. Phys. B* **29** 093101
[59] Hui T, Gui T X, Ping J Y, Xiang L Q and Hua L W 2019 *Acta Phys. Sin.* **68** 227701 (in Chinese)
[60] Qin F B, Qing H, Jun W, Jie Q M and Chao C J 2019 *Acta Phys. Sin.* **68** 240201 (in Chinese)
[61] Zhang H, Huang Y, Shi W Z, Zhou X H and Chen X S 2019 *Acta Phys. Sin.* **68** 207302 (in Chinese)
[62] Kuo W L and Li D F 2019 *Acta Phys. Sin.* **68** 193101 (in Chinese)
[63] Adams D J 1981 *Nature* **293** 447
[64] Hess B, Bekker H, Berendsen H J C and Fraaije J G E M 1997 *J. Comput. Chem.* **18** 1463
[65] Cornell W D, Cieplak P, Bayly C I, Gould I R, Merz K M, Ferguson D M, Spellmeyer D C, Fox T, Caldwell J W and Kollman P A 2002 *J. Am. Chem. Soc.* **117** 5179
[66] Alavi S and Ripmeester J A 2017 *Mol. Simul.* **43** 808
[67] Tian L L, Duan H M, Luo J M, Cheng Y H and Shi L 2021 *ACS Appl. Nano Mater.* **4** 9440
[68] Hess B, Kutzner C, van der Spoel D and Lindahl E 2008 *J. Chem. Theory Comput.* **4** 435
[69] Quigley D and Rodger P M 2008 *J. Chem. Phys.* **128** 154518
[70] Laio A, Rodriguez-Fortea A, Gervasio F L, Ceccarelli M and Parrinello M 2005 *J. Phys. Chem. B* **109** 6714
[71] Soper A K 2000 *Chem. Phys.* **258** 121
[72] Cao H, English N J and MacElroy J M 2013 *J. Chem. Phys.* **138** 094507
[73] Metzler R, Jeon J H, Cherstvy A G and Barkai E 2014 *Phys. Chem. Chem. Phys.* **16** 24128
[74] Ivanovskis G, Norman G E and Usmanova D R 2012 *Dokl. Phys.* **57** 427
[75] Chen Q, Moore J D, Liu Y C, Roussel T J, Wang Q, Wu T and Gubbins K E 2010 *J. Chem. Phys.* **133** 094501
[76] Alavi S, Udachin K and Ripmeester J A 2010 *Chemistry* **16** 1017
[77] Okuchi T, Takigawa M, Shu J F, Mao H K, Hemley R J and Yagi T 2007 *Phys. Rev. B* **75** 144104
[78] Strauss H L, Chen Z and Loong C K 1994 *J. Chem. Phys* **101** 7177
[79] Prisk T R, Hanna S and Azuah R T 2020 *J. Low Temp. Phys.* **201** 451
[80] Zhang Z, Wu T, Wang Q, Pan H and Tang R 2014 *J. Chem. Phys.* **140** 034706
[81] Kuhs W F, Staykova D K and Salamatin A N 2006 *J. Phys. Chem. B* **110** 13283
[82] Genov G, Kuhs W F, Staykova D K, Goreshnik E and Salamatin A N 2004 *Am. Mineral.* **89** 1228
[83] Salamatin A N, Lipenkov V Y, Hondoh T and Ikeda T 1999 *J. Phys. Chem. C* **29** 191
[84] Hjertenaes E, Trinh T T and Koch H 2016 *Phys. Chem. Chem. Phys.* **18** 17831
[85] Alavi S and Ripmeester J A 2007 *Angew. Chem. Int. Ed.* **46** 6102
[86] Frankcombe T J and Kroes G J 2007 *J. Phys. Chem. C* **111** 13044